

# Error- and Loss-Tolerances of Surface Codes with General Lattice Structures

Keisuke Fujii<sup>1</sup> and Yuuki Tokunaga<sup>2,3</sup>

<sup>1</sup>Graduate School of Engineering Science, Osaka University, Toyonaka, Osaka 560-8531, Japan

<sup>2</sup>NTT Information Sharing Platform Laboratories, NTT Corporation,

3-9-11 Midori-cho, Musashino, Tokyo 180-8585, Japan

<sup>3</sup>Japan Science and Technology Agency, CREST,

5 Sanban-cho, Chiyoda-ku, Tokyo 102-0075, Japan

We propose a family of surface codes with general lattice structures, where the error-tolerances against bit and phase errors can be controlled asymmetrically by changing the underlying lattice geometries. The surface codes on various lattices are found to be efficient in the sense that their threshold values universally approach the quantum Gilbert-Varshamov bound. We find that the error-tolerance of surface codes depends on the connectivity of underlying lattices; the error chains on a lattice of lower connectivity are easier to correct. On the other hand, the loss-tolerance of surface codes exhibits an opposite behavior; the logical information on a lattice of higher connectivity has more robustness against qubit loss. As a result, we come upon a fundamental trade-off between error- and loss-tolerances in the family of the surface codes with different lattice geometries.

*Introduction.*— Recently, topological order has attracted much interest in both condensed matter physics [1, 2] and quantum information science [3]. The ground state degeneracy of topologically ordered phase cannot be distinguished by local operations and hence robust against local perturbations. By encoding quantum information into such topologically degenerate subspaces, so-called topological quantum error correction (QEC) codes [3, 4], logical information can be protected from decoherence by repeated quantum error correction. There have been two types of the topological QEC codes, so-called surface codes [3] and color codes [4], both of which are the CSS (Calderbank-Shor-Steane) codes [5]. In both cases, the threshold values under perfect syndrome measurements have been calculated to be  $\sim 11\%$  [6, 7], which is close to the quantum Gilbert-Varshamov bound [5] in the limit of zero asymptotic rate with symmetric  $X$  and  $Z$  errors. In the case of the color codes, their performances have been compared among different lattice geometries, and their thresholds result in similar values  $\sim 11\%$  [7, 8]. This result is reasonable by considering the fact that the color codes are self-dual CSS codes, that is, they are symmetric under a Hadamard transformation. The surface codes, on the other hand, are not self-dual CSS codes, and hence it is possible to break the symmetry between properties of  $X$  and  $Z$  error-corrections. The surface code, however, has been intensively investigated so far only on the square lattice, which is a self-dual lattice, and therefore its error-correction properties are symmetric.

In this letter, we investigate the surface codes with general lattice geometries. Their constructions and error-correction procedures are basically the same as those of the original surface code. Since the stabilizer operators are not always symmetric under the duality transformation of the lattice (i.e. exchange of the vertexes and faces with each other), the error-tolerances of the surface codes with general lattice geometries are not always symmetric between  $X$  and  $Z$  errors. Interestingly, we find that such

asymmetry in the error-tolerance is related to the connectivity of the lattice which defines the surface; *error chains on a lattice of lower connectivity can be corrected easily*. Intuitively, this can be understood that finding appropriate pairs of incorrect error syndromes, which are the boundaries of the error chains, on the lattice of lower connectivity is easier, since the incorrect error syndromes are more isolated and less percolative. Furthermore, we find that the threshold values for independent  $X$  and  $Z$  errors exhibit a universal behavior; they, independent of the lattice geometries, approach the quantum Gilbert-Varshamov bound [5] in the limit of zero asymptotic rate with asymmetric  $X$  and  $Z$  errors. In this sense, the family of the surface codes can be said to be efficient. We also provide a recursive way to construct highly asymmetric surface codes on fractal-like lattices. In many experimental situations, dephasing is a dominant source of errors [9], and therefore the present family of asymmetric surface codes will help us to correct such biased noise efficiently.

The loss-tolerant scheme is based on a bond percolation phenomenon, where a reliable logical operator can be reconstructed even on the lossy surface as long as the survival probability of the qubits is higher than the bond percolation threshold [10]. Thus *the logical information on a lattice of higher connectivity is robust against qubit loss*. As a result, we come upon a fundamental trade-off between error- and loss-tolerances of the surface codes depending on the connectivity of the underlying lattices; the logical information on a lattice of higher connectivity is robust against qubit loss, but the error chains on such a lattice are difficult to correct (and vice versa). It is interesting to note that such a trade-off between error- and loss-tolerances has been also discussed in a far different situation [11].

*Surface codes on general lattices.*— Let us consider a lattice  $\mathcal{L}(E, V, F)$ , where  $E$ ,  $V$ , and  $F$  are the sets of edges, vertices, and faces of the lattice, respectively [see Fig. 1 (a)]. A qubit is associated with each edge. The

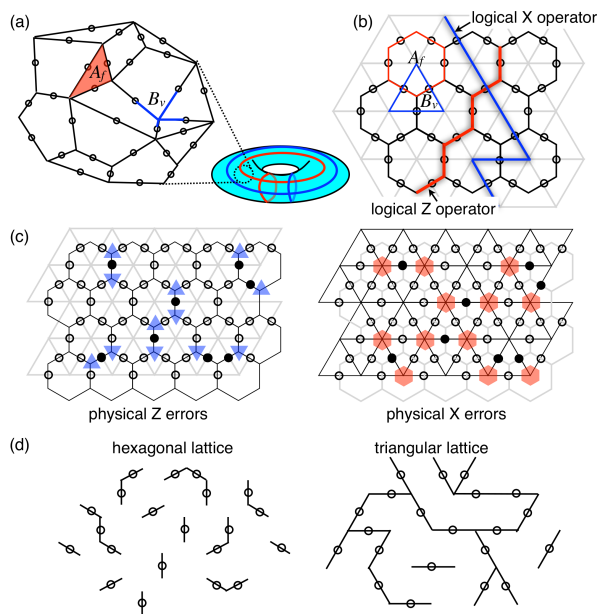


FIG. 1: (Color online) (a) A surface code with a general lattice structure. (b) The surface code on the hexagonal lattice and the logical operators. (c) Incorrect error syndromes against  $Z$  (left) and  $X$  (right) errors, which are associated with the chains on the primal and dual lattices respectively. Here, the  $Z$  (left) and  $X$  (right) errors are located at the same qubits depicted by the solid circles. (d) The remaining edges (qubits) on the primal (left) and dual (right) lattices after qubit loss. The logical  $Z$  and  $X$  operators are associated with the non-contractible loop on the primal and dual lattices, respectively.

stabilizer operators of the surface code on the lattice  $\mathcal{L}$  are defined for each face  $f \in F$  and vertex  $v \in V$ , respectively, as

$$A_f^{\mathcal{L}} = \bigotimes_{i \in E_f} Z_i, \quad B_v^{\mathcal{L}} = \bigotimes_{j \in E_v} X_j.$$

Here,  $Z_i$  and  $X_j$  denote Pauli operators on the  $i$ th and  $j$ th qubits ( $i, j \in E$ ) respectively, and  $E_f$  and  $E_v$  ( $E_{f,v} \subset E$ ) indicate the sets of edges which are surrounding the face  $f$  and are adjacent to the vertex  $v$ , respectively. From these definitions we define the lattice  $\mathcal{L}$  as primal. Its dual lattice, which is denoted by  $\tilde{\mathcal{L}}(\tilde{E}, \tilde{V}, \tilde{F})$ , can be defined by exchanging the vertices and faces of  $\mathcal{L}$  with each other. Similarly to the original surface code on the square lattice,  $Z$  and  $X$  errors are detected as incorrect error syndromes at boundaries of  $Z$  and  $X$  error chains on the edges of primal and dual lattices, respectively. The logical  $Z$  and  $X$  operators are defined as tensor products of Pauli  $Z$  and  $X$  operators on the non-contractible loops on the edges of the primal and its dual lattices [see Fig. 1 (b)], respectively. In the following, the logical operators play the following two roles: (i) If the error correction is failed, a logical operator acts on the code space, which we call a *logical error*. (ii) The logical operators represent encoded quantum information, which we

call *logical information*. Since  $H^{\otimes |E|} A_f^{\mathcal{L}} H^{\otimes |E|} = B_v^{\tilde{\mathcal{L}}}$ , the surface code defined on the primal lattice  $\mathcal{L}$  is equivalent to that defined on the dual lattice  $\tilde{\mathcal{L}}$  up to the Hadamard transformation  $H^{\otimes |E|}$ . In the case of the original surface code, which is defined on the square lattice, the  $Z$  and  $X$  error-tolerances are symmetric, since  $\mathcal{L} = \tilde{\mathcal{L}}$  up to translation.

Let us consider, for instance, a surface code on the hexagonal lattice as shown in Fig. 1 (b). In such a case,  $\mathcal{L} \neq \tilde{\mathcal{L}}$ , and hence the  $Z$  and  $X$  error-tolerances are no longer symmetric. Suppose that  $Z$  or  $X$  errors are, for example, located at those qubits depicted with solid circles in Fig. 1 (c). The  $Z$  and  $X$  errors are detected at the boundaries (vertices) of the error chains on the edges of the hexagonal (primal) and triangular (dual) lattices, respectively, which are denoted by blue (left) triangles and red (right) hexagons in Fig. 1 (c). In the error-correction procedure, we have to infer the locations of the errors from the information of incorrect error syndromes. As can be seen clearly from Fig. 1 (c),  $X$  errors (right) are less distinguishable than  $Z$  errors (left), since incorrect error syndromes are more dense and percolative. More precisely, the error syndromes of  $Z$  and  $X$  errors are associated with the vertices on the primal and dual lattices, respectively, and therefore the distinguishability of the  $Z$  and  $X$  errors depends on the connectivity of the primal and dual lattices, respectively. The bond-percolation threshold is one of the most well-known measures of the connectivity of lattices. The bond-percolation thresholds of the hexagonal (primal) and triangular (dual) lattices are given by 0.653 and 0.347, respectively. Since the hexagonal (primal) lattice has lower connectivity, the surface code on the hexagonal lattice is expected to be more robust against  $Z$  errors.

*Threshold values.*— In order to confirm the above observation, we perform numerical simulations and estimate the threshold values of the surface codes with various lattice geometries such as the Kagome, hexagonal, and  $(3,12^2)$  (*triangle-hexagonal*), say *tri-hexa*, lattices. For independent bit and phase errors with probability  $p_X$  and  $p_Z$ , respectively, topological error correction is simulated by using the minimum-weight-perfect-matching algorithm. Then, by using the finite-size scaling ansatz for the logical error probability,  $p_{Z,X}^l = A + B(p_{Z,X} - p_{Z,X}^{\text{th}})L^{1/\nu}$  with fitting parameters  $(A, B, \nu, p_{Z,X}^{\text{th}})$  similarly to Ref. [12], the threshold values  $p_Z^{\text{th}}$  and  $p_X^{\text{th}}$  against physical  $Z$  and  $X$  errors are calculated, respectively [13, 14]. The resultant threshold values are summarized in Table I. As we expected, when the lattice is not self-dual, the threshold values of the surface code exhibit asymmetry between  $Z$  and  $X$  errors, and their behavior under various lattices can be understood from the connectivity of the underlying lattices; if a primal lattice has lower connectivity (i.e. higher bond-percolation threshold), the corresponding surface code is robust against  $Z$  errors (i.e. higher threshold value  $p_Z^{\text{th}}$ ). On the other hand, in such a case, the dual lattice exhibits higher

lattice	$p_Z^{\text{th}}$	bond-percolation (primal)	$p_X^{\text{th}}$	bond-percolation (dual)
square	0.103	1/2	0.103	1/2
Kagome	0.116	0.524	0.095	0.476
hexagonal	0.159	0.653	0.065	0.347
tri-hexa	0.205	0.740	0.041	0.260

TABLE I: Summary of the threshold values of the surface codes on various lattices. The bond-percolation thresholds of the primal and dual lattices are also shown.

connectivity due to the Kesten's duality theorem (i.e. the sum of bond-percolation thresholds of a primal and its dual lattices is equal to one) [15]. Thus the threshold value of the  $X$  errors becomes lower [16]. Although there is no rigorous correspondence between the bond-percolation model and the topological error correction, it can be used as a good measure of the performance of the surface code.

In Fig. 2, these threshold values ( $p_X^{\text{th}}, p_Z^{\text{th}}$ ) are plotted with the quantum Gilbert-Varshamov bound  $R = 1 - h(p_X) - h(p_Z)$  in the limit of zero asymptotic rate  $R \rightarrow 0$ , where  $h(p)$  is the binary Shannon entropy [5]. Interestingly, for all lattices considered here, the threshold values ( $p_X^{\text{th}}, p_Z^{\text{th}}$ ) exhibit a universal behavior: they, independent of the lattice geometries, approach the bound. In this sense, the present family of the surface codes can be said to be efficient. Furthermore, the scaling exponents are obtained to be  $\nu \approx 1.5$  for all lattices, which indicates these surface codes belong to the same universality class as that on the square lattice [12]. From the above observation and these numerical evidences, it is expected in general that there is a trade-off between  $X$  and  $Z$  error-tolerances of the surface codes with other lattice geometries, and the trade-off is well characterized by the quantum Gilbert-Varshamov bound. Since the minimum-weight-perfect-matching algorithm is a sub-optimal decoding method, the threshold values will be improved by using more sophisticated decoding algorithms [10, 17].

There is an exact correspondence between the threshold values  $p^{\text{th}}$  of the surface code and the critical point of the random-bond Ising model on the Nishimori line  $e^{-2\beta_c} = p^{\text{th}}/(1 - p^{\text{th}})$  where  $\beta_c$  being the critical inverse temperature [3]. Thus, if the threshold value  $p_Z^{\text{th}}$  for the  $Z$  errors is higher, the corresponding random-bond Ising model on the primal lattice exhibits a higher critical temperature. On the other hand, in such a case, the threshold value  $p_X^{\text{th}}$  for the  $X$  errors is lower, and hence the critical temperature of the random-bond Ising model on the dual lattice becomes lower. According to the above result, the trade-off between the critical temperatures of the primal and dual lattices are also characterized by the Gilbert-Varshamov bound through the Nishimori temperature  $e^{-2\beta_c} = p^{\text{th}}/(1 - p^{\text{th}})$ .

*Loss-tolerance.* — Next we consider the performance of the surface codes against qubit loss. Recently, a novel loss-tolerant scheme has been proposed for the surface

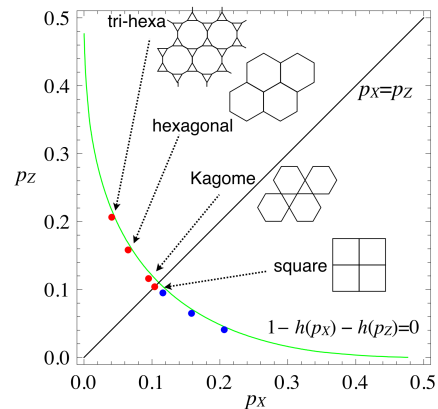


FIG. 2: (Color online) The threshold values ( $p_X^{\text{th}}, p_Z^{\text{th}}$ ) for the square, Kagome, hexagonal, and tri-hexa lattices are plotted (red dots) with the quantum Gilbert-Varshamov bound (green line). The blue dots are the threshold values for the surface codes defined on the duals of the Kagome, hexagonal, and tri-hexa lattices (from left to right).

code on the square lattice [10]. There, even if some qubits are lost, the stabilizer operators and the logical operators can be reconstructed as long as the loss rate is less than a threshold. The threshold value of qubit loss without errors is given exactly by the bond-percolation threshold of the lattice. This is because one can reconstruct a logical operator as long as the remaining qubits (bond) percolate through the lossy surface [see Fig. 1 (d)]. We can also apply the loss-tolerant scheme for the surface codes on the general lattices in a similar manner as in Ref. [10]. Then, the loss-tolerances of the logical  $X$  and  $Z$  information also become asymmetric depending on underlying lattice geometries. According to the Kesten's duality theorem, there is a trade-off between the bond-percolation thresholds of the primal and dual lattice. Thus, asymmetry in the tolerable loss rates  $p_X^{\text{loss}}$  and  $p_Z^{\text{loss}}$  of the logical  $X$  and  $Z$  information, respectively, is subject to a trade-off,  $p_X^{\text{loss}} + p_Z^{\text{loss}} = 1$ .

We also perform numerical simulations for the loss-tolerant scheme on the Kagome, hexagonal, and tri-hexa lattices. The resultant threshold curves ( $p^{\text{loss}}, p^{\text{th}}$ ) of the error and loss rates are plotted in Fig. 3 (a) for each lattice for logical  $X$  and  $Z$  information. The logical  $X$  information is robust against both  $Z$  errors and qubit loss as shown in Fig. 3 (a), while the logical  $Z$  information is

fragile against both  $X$  errors and qubit loss [16]. These results can be understood from the two trade-offs, which we have studied above, the trade-off between the  $Z$  and  $X$  error-tolerances [points on the vertical axis in Fig. 3 (a)], and the trade-off between the loss-tolerances of logical  $Z$  and  $X$  information [points on the horizontal axis in Fig. 3 (a)]. If we choose the primal lattice  $\mathcal{L}$  of low connectivity so that the surface code is robust against  $Z$  errors [see Fig. 1 (c) left], then the bonds of such a primal lattice are less percolative, and hence the logical  $Z$  information becomes fragile against loss [see 1 (d) left]. This is also the case for fragility against  $X$  errors and robustness of the logical  $X$  information [see Fig. 1 (c) right and (d) right]. That is, there is a fundamental relationship between robustness against errors and fragility of the logical information against qubit loss depending on the lattice geometries of the surface codes.

*Systematic construction of asymmetric lattices.*— In the above case, qubit loss occurs randomly according to the loss rate  $p^{\text{loss}}$ . It is also suggestive to consider a systematic qubit loss. If we introduce a systematic qubit loss for the triangular (dual of the hexagonal) lattice, whose threshold value is 15.9% as shown in Table I, then we can reconstruct the surface as the square lattice, whose threshold value is 10.3% [see Fig. 3 (b)  $\mathcal{L}_0$  and  $\mathcal{L}_1$ ]. By doing the inverse operation of the systematic qubit loss, namely, a systematic injection of qubits, we can construct a new lattice  $\mathcal{L}_n$  recursively, which has high connectivity (its dual lattice  $\tilde{\mathcal{L}}_n$  has low connectivity), as shown in Fig. 3 (b). Therefore, the threshold value for the  $Z$  ( $X$ ) errors on  $\tilde{\mathcal{L}}_n$  ( $\mathcal{L}_n$ ), which has lower (higher) connectivity, is expected to be higher (lower) than that of  $\tilde{\mathcal{L}}_{n-1}$  ( $\mathcal{L}_{n-1}$ ). On the other hand, the logical  $Z$  ( $X$ ) information is more fragile (robust) against qubit loss.

*Conclusion and discussion.*— We have investigated the surface codes with general lattice geometries. These surface codes are efficient, since their threshold values approach the quantum Gilbert-Varshamov bound universally. We have found that there are interesting relationships between error or loss-tolerances of the surface codes and the geometrical properties of the underlying lattices, where the connectivity of the lattice has an opposite effect in error and loss-tolerances. This results in a fundamental trade-off between robustness against errors and fragility of the logical information against qubit loss (and vice versa) among the surface codes on the different lattices. We also provide a recursive way to construct a highly asymmetric surface code on a fractal-like lattice. These results suggest that we can systematically find an efficient surface code by selecting the underlying lattice geometry depending on the degree of biased noise.

The surface codes with general lattice geometries also support topologically protected measurement-based quantum computation by braiding the defects [19, 20]. The error- and loss-tolerances in fault-tolerant topological quantum computation on the general lattices are an intriguing future problem.

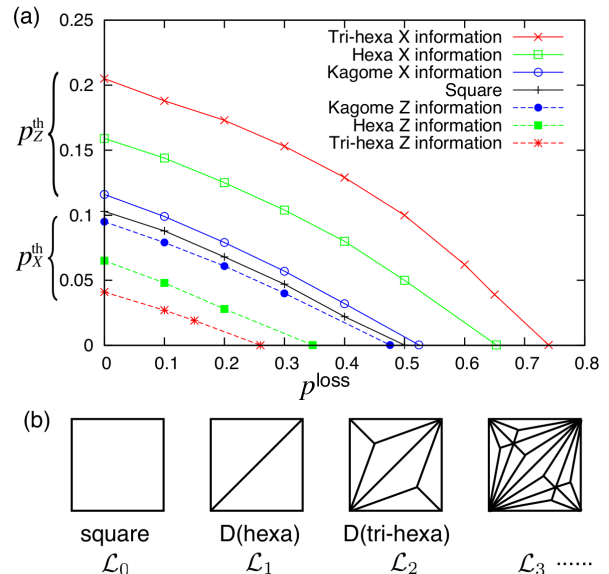


FIG. 3: (Color online) (a) The threshold curves ( $p^{\text{loss}}, p^{\text{th}}$ ) for logical  $X$  (solid line) and  $Z$  (dotted line) information [18]. Top to bottom: tri-hexa ( $X$ ), hexagonal ( $X$ ), Kagome ( $X$ ), square ( $X$  and  $Z$ ), Kagome ( $Z$ ), hexagonal ( $Z$ ), and tri-hexa ( $Z$ ). (b) A recursive way to construct a fractal-like lattice  $\mathcal{L}_n$  of higher connectivity. Its dual lattice  $\tilde{\mathcal{L}}_n$  has lower connectivity.

It is an interesting correspondence that a trade-off between error- and loss-tolerances has been found also in a far different situation [11], where lost information is recovered by using counter-factual indirect measurements on a specific shape of the cluster states. In such a case, if we introduce more redundancy for the loss-tolerance, more errors are accumulated, which results in a similar trade-off. This correspondence suggests that there might be more fundamental principle between error- and loss-tolerances; *for two mutually noncommuting observables, if one observable is robust against qubit loss, the other one must be fragile against environmental perturbations* [21].

KF is supported by MEXT Grant-in-Aid for Scientific Research on Innovative Areas 20104003.

*Note added.*— During preparation of this manuscript [22], a related work has been appeared [23], which also supports generality of the present results.

- 
- [1] X.-G. Wen and Q. Niu, Phys. Rev. B **41**, 9377 (1990).
  - [2] S. D. Sarma, M. Freedman, and C. Nayak, Physics Today, July 2006, pag. 32.
  - [3] A. Yu. Kitaev, Ann. Phys. **303**, 2 (2003).
  - [4] H. Bombin and M. A. Martin-Delgado, Phys. Rev. Lett. **97**, 180501 (2006); H. Bombin and M. A. Martin-Delgado, Phys. Rev. Lett. **98**, 160502 (2007).
  - [5] A. R. Calderbank and P. W. Shor, Phys. Rev. A **54**, 1098 (1996); A. M. Steane, Phys. Rev. Lett. **77**, 793 (1996).
  - [6] E. Dennis, A. Yu. Kitaev, and J. Preskill, J. Math. Phys.



- 43**, 4452 (2002).
- [7] H. G. Katzgraber, H. Bombin, and M. A. Martin-Delgado, Phys. Rev. Lett. **103**, 090501 (2009).
- [8] M. Ohzeki, Phys. Rev. E **80**, 011141 (2009).
- [9] P. Aliferis, F. Brito, D. P. DiVincenzo, J. Preskill, M. Steffen, and B. M. Terhal, New J. Phys. **11**, 013061 (2009).
- [10] T. M. Stace, S. D. Barrett, and A. C. Doherty, Phys. Rev. Lett. **102**, 200501 (2009); T. M. Stace and S. D. Barrett, Phys. Rev. A **81**, 022317 (2010); S. D. Barrett and T. M. Stace, Phys. Rev. Lett. **105**, 200502 (2010).
- [11] P. P. Rohde, T. C. Ralph, and W. J. Munro, Phys. Rev. A **75**, 010302(R) (2007).
- [12] C. Wang, J. Harrington and J. Preskill, Ann. Phys. **303**, 31 (2003).
- [13] Here, the logical error probabilities  $p_{Z,X}^l$  mean that after the recovery operations logical  $Z$  and  $X$  operators act on the code space with probabilities  $p_{Z,X}^l$ , respectively. If a logical  $Z$  ( $X$ ) error occurs, the logical  $X$  ( $Z$ ) information is flipped, since the logical operators anticommute. If  $p < p_Z^{\text{th}}$  ( $p < p_X^{\text{th}}$ ), the probability  $p_{Z,X}^l$  ( $p_{X,Z}^l$ ) of such a logical  $Z$  ( $X$ ) error is suppressed rapidly by increasing the lattice size  $L$ .
- [14] The numerical simulations are performed on the  $L \times L$  lattice with  $L = 16, 24, 32$  for the square lattice. For other structures, the lattices of the similar numbers of qubits are used.
- [15] H. Kesten, *Percolation Theory for Mathematicians* (Birkhäuser, Boston 1982).
- [16] It is, of course, possible to construct surface codes, which are robust against  $X$  errors, by defining their stabilizer operators on the duals of the Kagome, hexagonal, and tri-hexa lattices as shown in Fig. 2. This is also the case for the loss-tolerance, where the logical  $Z$  information becomes robust against qubit loss in the surface codes defined on these duals.
- [17] G. Duclos-Cianci and D. Poulin, Phys. Rev. Lett. **104**, 050504 (2010).
- [18] When  $p^{\text{loss}}$  is near the bond percolation threshold, the numerically obtained  $p^{\text{th}}$  lies below the drawn curve (not shown in Fig. 3), because the finite size effects become dominant, and therefore the universal scaling law breaks down similarly to the case of the square lattice [10].
- [19] R. Raussendorf and J. Harrington, Phys. Rev. Lett. **98**, 190504 (2007); R. Raussendorf, J. Harrington, and K. Goyal, New J. Phys. **9**, 199 (2007).
- [20] R. Raussendorf, J. Harrington, and K. Goyal, Ann. of Phys. **321**, 2242 (2006).
- [21] This provides an intuitive understanding of difficulty to observe superposition of macroscopically distinct two quantum states, i.e., the Schrödinger's cat paradox.
- [22] The preliminary version of this work was presented at QIP 2012 conference held in Dec. 2011.
- [23] B. Röthlisberger, J. R. Wootton, R. M. Heath, J. K. Pachos, and D. Loss, arXiv:1112.1613.